Contents lists available at Science-Gate

International Journal of Advanced and Applied Sciences

Journal homepage: http://www.science-gate.com/IJAAS.html

An antenna synthesis of integrated primary and secondary surveillance radar

Tomas Zalabsky*, Tomas Shejba, Vladimir Schejbal, Pavel Bezousek, Milan Chyba

Faculty of Electrical Engineering and Informatics, University of Pardubice, Pardubice, Czech Republic

ARTICLE INFO

Article history:
Received 27 December 2015
Received in revised form
23 January 2016
Accepted 23 January 2016

Keywords:
Primary surveillance radar
Secondary surveillance radar
Integrated antenna
Antenna synthesis

ABSTRACT

The paper deals with a new concept of an integrated antenna array for air traffic control (ATC). The antenna consists of 3D primary surveillance radar (PSR) and secondary surveillance radar (SSR). There is a detailed description of integration of antennas, used synthesis techniques and comparison of measurements for both radars. Numerical simulations including random errors of amplitudes and phases on each output of feeding network and their effect on radiation patterns are presented again for both radars. Furthermore an analysis of failure in PSR feeding network and final effect on radiation pattern is presented.

1. Introduction

Typical construction of existing surveillance radars for air traffic control is based on separation of primary radar (PSR) antenna and secondary radar (SSR) antenna. The PSR antenna is typically situated under the SSR antenna with a common rotation axis (Oliner et al., 2007), (Bezousek and Schejbal, 2004), (Milligan, 2005) and (Skolnik, 2008). This configuration is applicable only in the case of a small vertical aperture of a SSR antenna. Recently in both radars, large vertical apertures are preferred (Oliner et al., 2007) due to their higher gain and lower earth reflection. However, installation of two antennas with very high aperture above each other on one common mast could result in suffering from mechanical instability and electrical troubles in adverse weather and from transportation difficulties in the case of a mobile system. Enumerated reasons lead to integration of both antennas into one.

In the past, integration of both antenna systems using separate feeders, common reflectors or various combinations of reflectors and dipole antenna arrays were reported (Bezousek and Schejbal, 2004), (Duppressor, 1983), (Cohen, 1983). In this paper the synthesis of 3D PSR and monopoles SSR antenna radiation patterns are described. Antenna integration is based on combination of slotted waveguides and patch arrays (see Fig. 1). Dual frequency or broadband array antennas based on a combination of patch and slotted waveguides, were also described in (Uher et al., 1997; Stasiowski and Schaubert, 2008).

The primary radar antenna working in S band (2.7 – 2.9 GHz) consist of 32 equidistant spaced horizontal polarized slotted waveguide rows, each with 77 radiating slots (again equidistant spaced) of alternating slope for suppression of vertical polarization. The redundant emitted vertical polarization is suppressed by vertical conducting diaphragms between slots made by hollow metals fins. Vertical conducting plates also suppress mutual coupling between each element in waveguide. The second advantage of these fins is that together with slotted waveguides create a very robust, resident and self-supporting mechanical construction. Each of the waveguide rows are equipped by their own receiver and transceiver module. This solution allows creation of a desired radiation pattern in a vertical plane (by signal distribution network) and creates several beams on the receiver side (digitally) which results in possibility to determinate elevation angle of targets. The antenna structure was described in more detail in (Bezousek et al., 2013; Bezousek, Chyba et al., 2013; Bezousek et al., 2014).

The secondary surveillance radar antenna consists of 27 vertical radiation columns. The vertical feeders are located inside the hollow metals fins between waveguide slots. For this purpose each third metal fin is used. On the front side of these fins are situated radiating elements – patches, which are tuned to the required frequencies 1030 MHz and 1090 MHz. As these SSR radiators and vertical feeders are situated in front of the primary antenna slots their forms, dimensions and positions are very critical for a high PSR antenna quality. The design was described in (Zalabsky, 2012; Schejbal et al., 2013; Bezousek and Schejbal, 2011).

* Corresponding Author.
Email Address: tomas.zalabsky@student.upce.cz

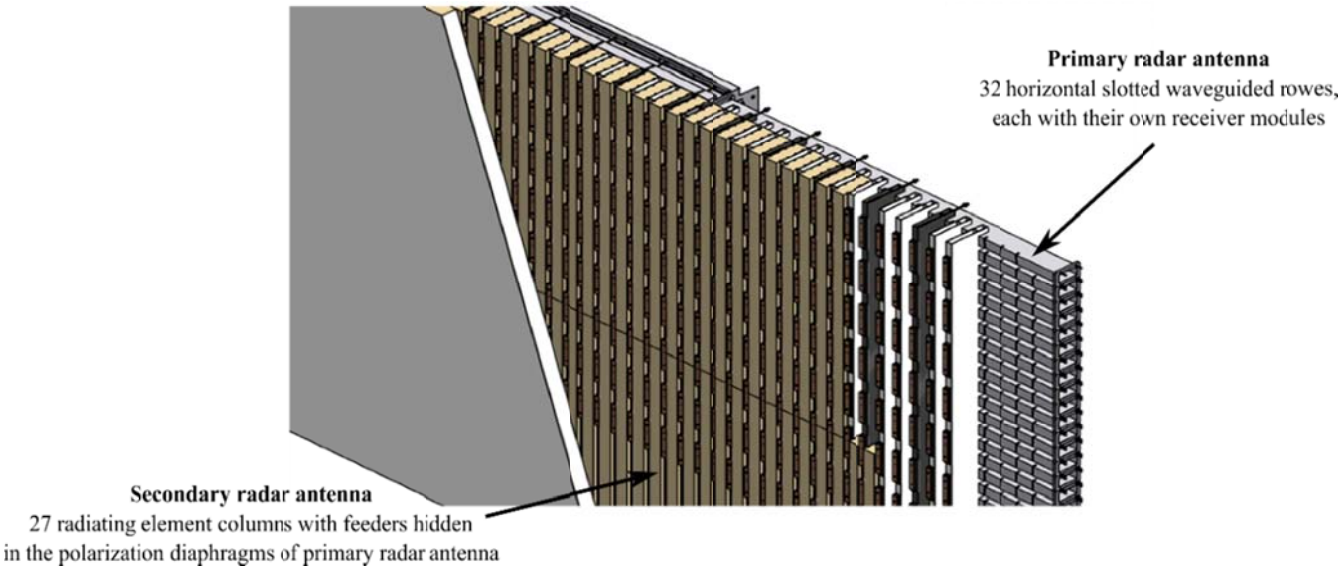

Fig. 1: Concept of integration of primary and secondary antenna array

2. Primary surveillance radar antenna

The radiation pattern of the PSR antenna is created by 77 slots in a waveguide for the horizontal plane (Fig. 2a) and by 32 horizontal slotted waveguides for the vertical axis (Fig. 2b). Amplitude distribution for the horizontal axis is obtained from the Taylor distribution with theoretical side lobe level 45 dB. Phases are without beam squint zero.

The vertical radiation pattern has the shape of a squared cosecant (Barton and Leonov, 1997). It is done by phase shifts obtained by phase synthesis (Shejbal, 2012). Final phases obtain a beam squint of 10 degrees at a lower elevation (antenna is 10 degrees tilted). Each phase shift is realized by a different length of the feeding distribution network. All rows are then fed by equal amplitudes and a radiation pattern is formed by phases only. It is useful since it is possible to use only one transmitter type for all waveguide rows (easier design, lower cost, easier maintenance).

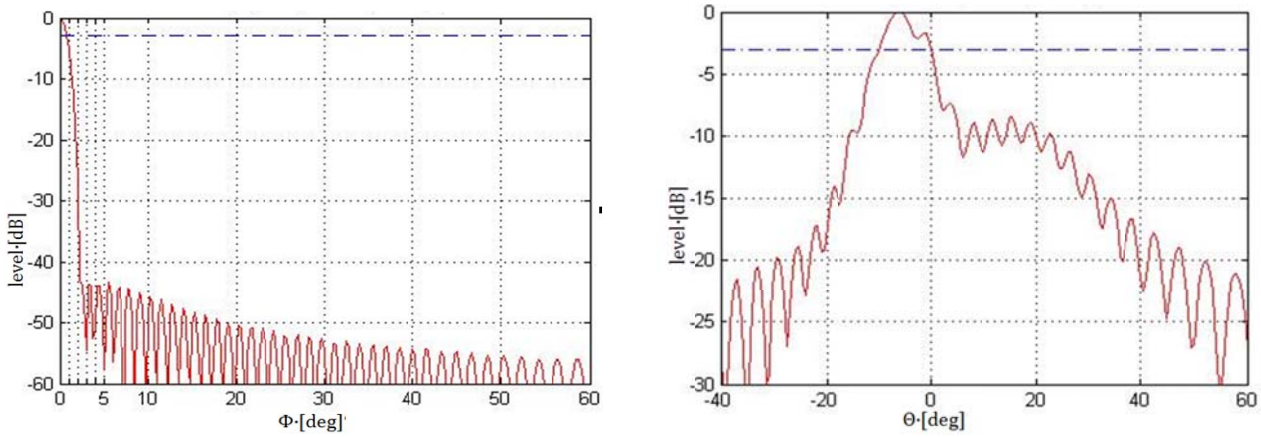

a: Horizontal b: Vertical

Fig. 2: Array factor for PSR antenna at center frequency

As mentioned above, slotted waveguides have equidistant inter element spacing which was calculated for a center frequency (2.8 GHz). In the case of frequency shift (in our application PSR works in 200 MHz bandwidth) wavelength is changed, but slot distance (of slotted waveguide) is still constant. It leads to beam squint, because waveguide rows are serial fed. Patterns comparison for start, center and stop band frequencies are shown in Fig. 3. Horizontal patterns are obtained by measurement in near zone and are calculated to far zone. In the case of frequency shift of 100 MHz the main lobe moves about 3.52 degrees.

In the case of the vertical diagram, there are feeding manifolds where each phase shift is done by changing the length of the strip line. Frequency change then leads to phase shift on each waveguide row. Phases of each row are independent of each other, so frequency shift does not lead to beam squint, but to modification of the radiation pattern. Fig. 3b t shows each computed array factor with directivity of radiating element. There are only small differences with frequency change.

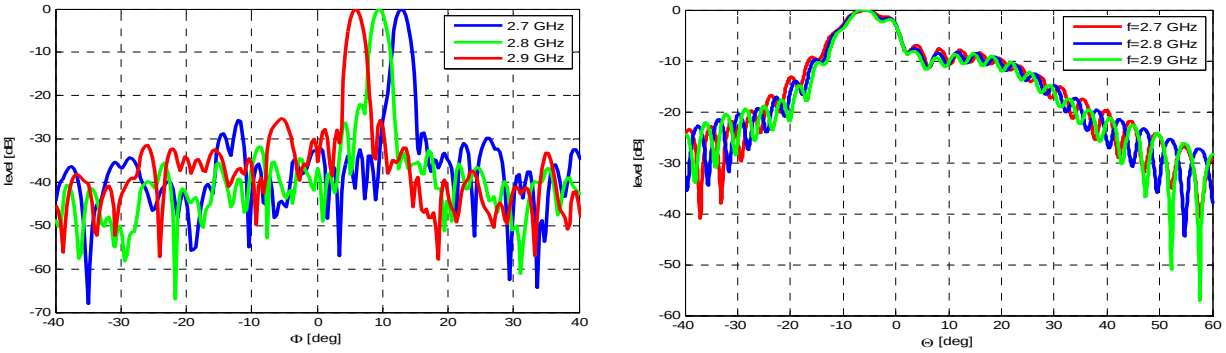

a: Horizontal b: Vertical

Fig. 3: Patterns comparison at each frequency

3. Receivers' beams

The azimuth pattern is same for transmitting and receiving (Fig. 2a). The transmitting pattern (Fig. 2b) has a squared cosecant shape to elevation 45° on the vertical axis. The receiving pattern (Fig. 4 normed to beam without beam squint) is not the same; there are eight receiving beams digitally formed in a digital beam forming processor. There sum Σ and diff Δ patterns from 32 waveguide rows are formed.

Sum pattern beam width is not the same for all eight beams. It is narrower for low elevation and wider for higher elevation. Most objects are far from PSR (low elevation) and we need to separate them in angle. A contrary object, close to PSR, has high elevation and there are not so many of them and beam width can be wider. If PSR is situated in the airport, there are other radar systems (e.g. (Moorcroft, 1958)), which are used for accurate determination of elevation angle. The sum pattern beam width (3dB) is 3.4 deg without beam squint with using all 32 rows. We achieve wider beam width by using lower number of rows for digital beam forming.

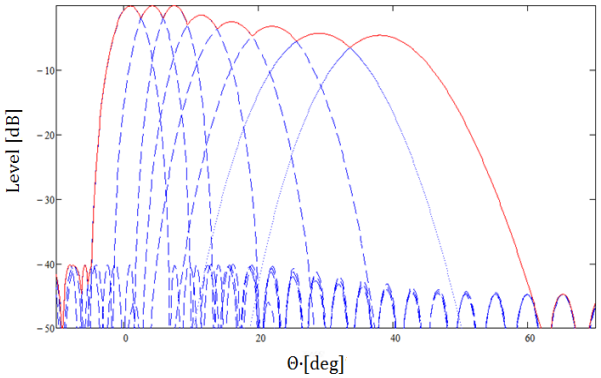

Fig. 4: Receiving beams digitally formed in digital beam forming processor (center frequency)

4. Random errors

In case of random amplitudes and phase changes on individual radiators, the radiation pattern is different from the radiation pattern observed with computed amplitudes and phases. There are several aspects which can perform on radiation pattern, e.g.: amplitude and phase errors in feeding circuits, radiating elements, mechanical constructions, etc. Amplitude and phase errors remove part of the energy from the main lobe and scatter this energy to side lobes. The scattered energy for small uncorrelated errors is: $\sigma_T^2 = \sigma_\varphi^2 + \sigma_A^2$ where σ_φ, σ_A are amplitude and phase standard deviation errors. This energy is radiated to far zone by radiator gain influence. Mean-squared side lobe level is determined as follows:

$$MSSL = \frac{\sigma_T^2}{\eta_a N(1-\sigma_T^2)} \quad (1)$$

Where: N – number of elements in array,

η_a – aperture efficiency.

Amplitude errors are multiplied with individual amplitudes. Phase errors are added to theoretical phases. Influenced radiation pattern by random amplitude and phase errors for PSR is shown in Fig. 6 for σ_A = 0.83 dB, σ_φ = 5.7 deg and four realizations.

The main lobes of horizontal patterns are the same for all scenarios. Difference is on the side of the side lobes, but still under -35 dB). The vertical pattern is more dependent (compare to horizontal pattern) on phase errors because the radiation pattern is only formed by phase shifts between each radiator. Amplitudes of each radiator are equal. Fig. 5 shows radiation pattern with failure in feeding of 10th waveguide row.

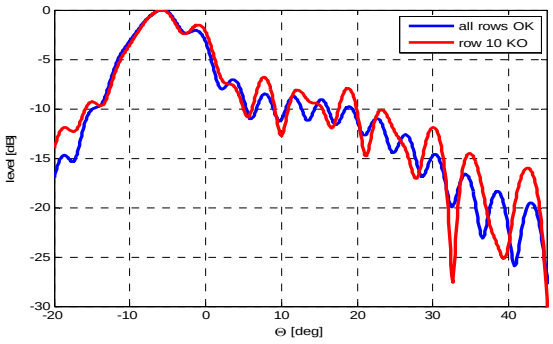

Fig. 5: Comparison of the vertical radiation pattern and radiation pattern with feed failure of 10th row at center frequency for PSR antenna

Influenced radiation pattern by random amplitude and phase errors for SSR is shown in Fig. 7 for σ_A = 0.83 dB, σ_φ = 5.7 deg and four realizations.

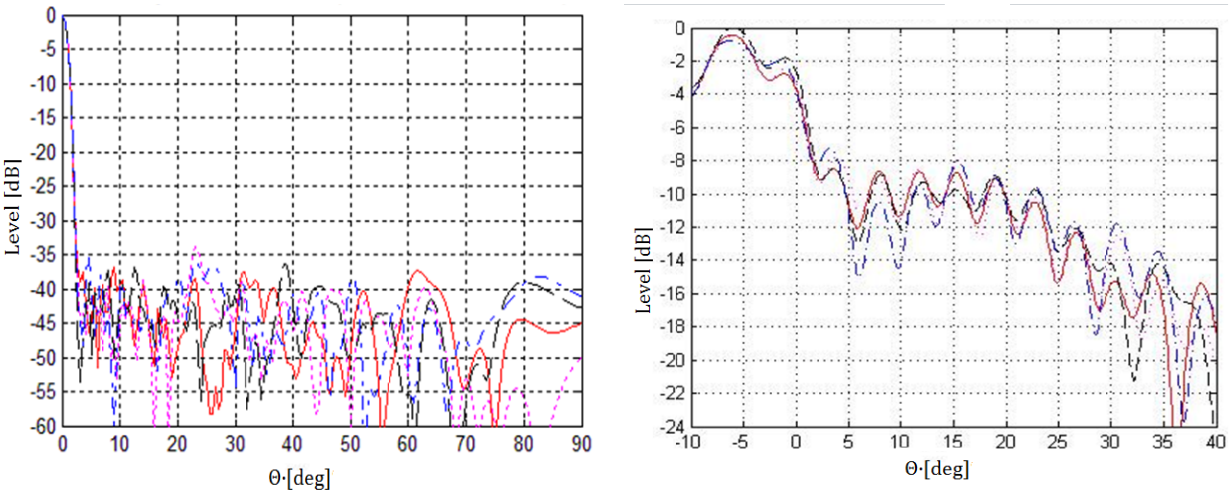

a: Horizontal b: Vertical

Fig. 5: Numerical simulation of radiation patterns for PSR antenna at center frequency

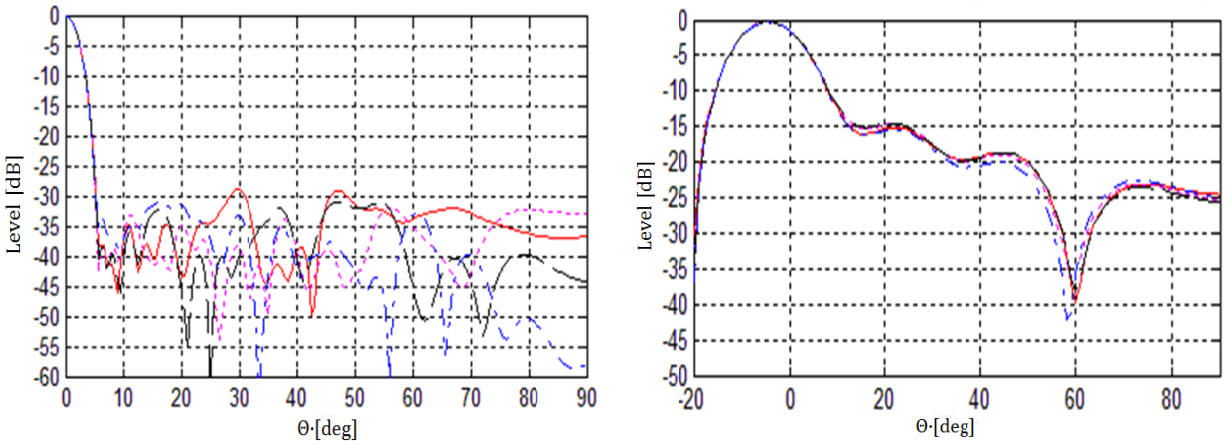

a: Horizontal b: Vertical

Fig. 7: Numerical simulation radiation patterns for SSR antenna at center frequency

5. Measured radiation patterns of SSR

After realization of whole antenna structure the real radiation patterns of secondary surveillance radar has been measured. Measurements were performed in an anechoic chamber using near field measurements method. The measured radiation pattern of all 3 beams (SUM, DIFF, OMEGA) at frequency 1.03 GHz in horizontal plane are shown in the Fig. 8.

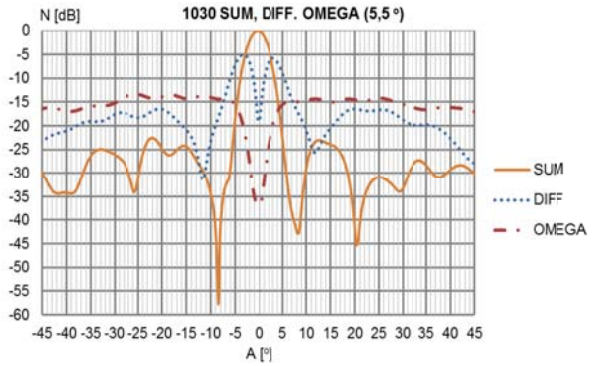

Fig. 8: Diagrams of SSR antenna at frequency 1030 MHz in horizontal plane

It is obvious that the measured radiation patterns well correspond to the proposed waveforms.

The measured radiation pattern of secondary surveillance radar in vertical plane is shown in the Fig. 9.

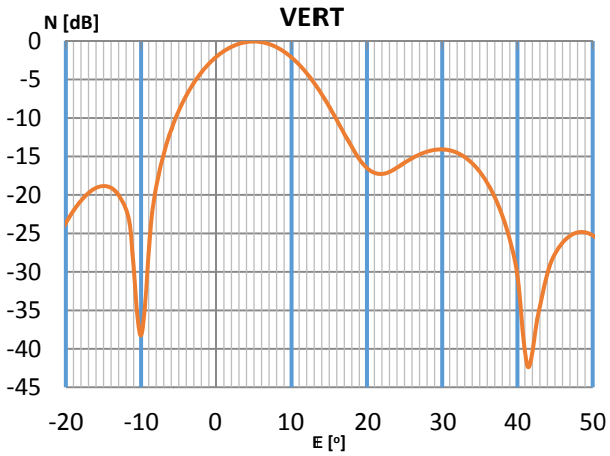

Fig. 9: Vertical radiation pattern of the SUM beam of SSR antenna at frequency 1030 MHz.

It is evident that the shape of measured radiation pattern well corresponds with required cosecant squared course; the comparison of measured values with required has been performed and complements this contribution.

6. Conclusion

In this paper the concept of integration of PSR and SSR antenna was briefly described. The presented antenna structure offers good high frequency parameters of both antennas at two frequency bands at a low antenna height, beneficial mainly in mobile application. The radiation pattern shapes for both plane (horizontal and vertical) and for both radar systems (PSR and SSR) were discussed. A synthesis of a new planar phased active array of 3-D PSR, without compromise regarding the antenna parameters, with the Taylor distribution for horizontal pattern, transmitted shaped fan beam and eight receiving beams, is provided. Both numerical simulations including random errors of amplitudes and phases as well as non-working transmitting row are presented. Finally, the proposed antennas radiation pattern has been verified via real measurement using near field technic. It can be summarized that the designed antenna system complies with our application for air traffic control system

Acknowledgement

The described research was supported by the Technology Agency of the Czech Republic, project No. TA03031548.

References

Barton DK, Barton DK and Leonov SA (1997). Radar technology encyclopedia. Artech House, Inc, Norwood, USA.

Bezousek P and Schejbal V (2004). Radar technology in the Czech Republic. Aerospace and Electronic Systems Magazine, IEEE, 19(8): 27-34.

Bezousek P and Schejbal V (2011). Monopulse Secondary Surveillance Radar Antenna for Air Traffic Control. Perners Contact, 5(5): 21-28.

Bezousek P, Chyba M, Schejbal V and Pidanic J (2013, April). Dual frequency band integrated antenna array. In Antennas and Propagation (EuCAP), 2013 7th European Conference on (pp. 2137-2141). IEEE.

Bezousek P, Chyba M, Schejbal V, Karamazov S, Zalabsky T and Cernik L (2014, August). Combined antenna array for primary and secondary surveillance radars. In Antennas and Propagation in Wireless Communications (APWC), 2014 IEEE-APS Topical Conference on (pp. 597-600). IEEE.

Bezousek P, Schejbal V, Chyba M, Bazant P, Krcmar V and Cernik L (2013). Integrated PSR/MSSR Antenna Array. Proc. of the Int. Conf. on Military Technologies 2013, Brno: 525 –534

Cohen G (1983) Antenna for Primary and Secondary Radars, US Pat. 4376937.

Dupressoir, A. (1983). U.S. Patent No. 4,400,701. Washington, DC: U.S. Patent and Trademark Office.

Milligan TA (2005). Modern antenna design. John Wiley and Sons. John Wiley & Sons, New York, USA.

Moorcroft GJ (1958). Precision approach radar. Proceedings of the IEE-Part B: Radio and Electronic Engineering, 105(9S): 344-350.

Oliner AA, Jackson DR and Volakis JL (2007). Antenna engineering handbook. McGraw Hill, New York, USA.

Schejbal V, Bezousek P, Pidanic J and Chyba M (2013). Secondary Surveillance Radar Antenna [Antenna Designer's Notebook]. Antennas and Propagation Magazine, IEEE, 55(2): 164-170.

Shejbal T (2012). Signal distribution network for phased antenna array of a primary radar. Ph.D. Thesis, University of Pardubice.

Skolnik MI (2008) Radar Handbook. McGraw Hill, New York, USA.

Stasiowski M and Schaubert D (2008, September). Broadband array antenna. In Proceedings of the 2008 Antenna Applications Symposium (pp. 42-59).

Uher J and Pokuls R (1997). U.S. Patent No. 5,661,493. Washington, DC: U.S. Patent and Trademark Office.

Zalabsky T (2012). Horizontal signal distribution network for a phased antenna array of secondary radar. Ph.D. Thesis, University of Pardubice.